arXiv:1112.3664v1 [quant-ph] 15 Dec 2011

Measuring Probabilities which Violate "Reality" in a Bell Inequality Experiment

B. L. Higgins,[1, 2] M. S. Palsson,[1] G. Y. Xiang,[1, 3] H. M. Wiseman,[1] and G. J. Pryde[1]

[1] *Centre for Quantum Dynamics and Centre for Quantum Computation and Communication Technology, Griffith University, Brisbane 4111, Australia*

[2] *Institute for Quantum Computing, University of Waterloo, Waterloo, ON N2L 3G1, Canada*

[3] *Key Laboratory of Quantum Information, University of Science and Technology of China, Hefei 230026, China*

Bell inequalities limit measurable correlations between properties of two physical systems, under two assumptions: that these properties can be ascribed independent of measurement, and that influences between them are bounded by light-speed propagation. Certain quantum entangled systems do not submit to this *local realistic* description, illustrated by copious experimental tests. Usually, to avoid quantum mechanical measurement back-action, different measurements are made on each of several subensembles of identical quantum systems. Here we show that weak measurements, which avoid back-action by weakly coupling the measurement device to the system, can be used to identically measure all quantum systems in the ensemble, providing a direct empirical footing from which to reason about their properties. The quantum mechanical violation of Bell inequalities is explained by the negative weak-valued probabilities that we measure, compatible with an operational physical model which preserves locality at the expense of objective realism.

Entanglement is the most striking property of quantum physics, providing a resource for quantum information technologies [1–5] and leading to highly counterintuitive effects in the laboratory. Specifically, measurements on bipartite entangled systems demonstrate a contradiction with the notion that systems have properties that are locally describable, independent of measurement, as first discussed by Einstein, Podolsky and Rosen (EPR) [6]. Following the proof that this notion—formalized as the joint assumption of locality and realism—leads to empirically testable Bell inequalities [7], many experiments (e.g. refs [8–14]) have demonstrated that at least one of these assumptions must be false, contrary to our strong classical intuition.

Tests of Bell inequalities typically involve measuring two pairs of observables, one pair on each system. However, because the observables in each pair are complementary (e.g. spin projections $\hat{\sigma}_X = \hat{X}$ and $\hat{\sigma}_Z = \hat{Z}$ of a quantum bit), measurement back-action makes it impossible to simultaneously measure all four combinations of observables on a given bipartite system. Rather, only one of the four combinations can be measured on each instance of the state. The inferences about the non-local-realism of the particles' descriptions come from the probabilities of outcomes on *different* sets of measurements on four different (albeit nominally equivalent) subensembles of quantum systems.

Here we use weak measurements of polarization-entangled photons, and the formalism of weak values, to empirically determine joint probabilities for the simultaneous values of complementary observables. In weak measurements, measurement back-action can be made arbitrarily small by reducing the strength of the coupling between the measurement probe and the system. Thus, it is possible to perform a weak measurement of one observable ($\hat{Z}$, for example) followed by a strong measurement of a complementary observable (e.g. $\hat{X}$) on the same particle; the same technique can be utilized on the second particle (Figure 1). Although the results of weak measurements have a large variance due to the weak coupling, a good signal to noise ratio can be achieved by averaging over a sufficiently large ensemble. Because the same measurements can be applied to all members of the ensemble, this technique provides an *observationally grounded* method from which to infer properties of the quantum systems between preparation and the final strong measurements [15]. Our method is similar to that recently used in inferring the trajectories [16, 17] and wavefunctions [18] of single photons in a double-slit interferometer. In the present case, our method allows us to examine the consistency of measurement results with a local but non-realistic description of the entangled state as introduced by Hofmann [19], providing a new perspective on Bell inequalities.

We gain new insights into quantum correlations and the foundations of quantum mechanics by applying weak measurements to the well-known Clauser–Horne–Shimony–Holt (CHSH) version [20] of Bell inequality. The CHSH inequality can be written as a bound on the expectation value of the CHSH parameter, which is a function of measurement result correlations between two systems. The CHSH parameter depends on the outcomes of *two* measurements on each of the systems:

$$S_{\text{CHSH}} = (X + Z)P + (X - Z)Q, \tag{1}$$

where $X, Z \in \{\pm 1\}$ are the results of a pair of measurements on a system A (Alice's system), and $P, Q \in \{\pm 1\}$ similarly for a system B (Bob's system). Assuming locality, we can evaluate the expectation of this by summing over the 16 possible combinations of measurement outcomes,

$$\langle S_{\text{CHSH}} \rangle = \sum_{X,Z,P,Q} [(X + Z)P + (X - Z)Q] \Pr[X, Z, P, Q]. \tag{2}$$

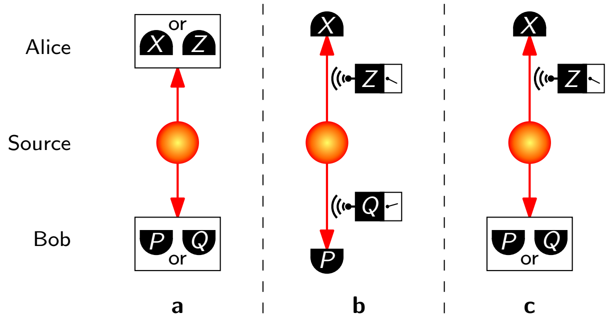

FIG. 1: Measurements in Bell inequality tests. A source provides a pair of (possibly correlated) systems, one each to Alice and Bob, who each measure one out of two possible observables. Traditionally (**a**) Alice and Bob each choose one or the other observable to measure strongly for each system. Using weak measurements (**b**) no such choice is necessary, as Alice and Bob may collect statistics of every observable with a fixed configuration. Doing so, Alice and Bob may infer probabilities for simultaneous outcomes that cannot be measured directly. Alternatively (**c**), Alice may perform weak measurements while Bob performs strong measurements. Configurations **b** and **c** generate identical results owing to the factorization of the CHSH parameter (see text).

Notice that only one of $(X+Z)P$ or $(X-Z)Q$ contributes to each term of the sum because one must be zero. If the probability of each outcome is *realistic*, i.e. $0 \leq \Pr[X,Z,P,Q] \leq 1$, it is simple to arrive at the CHSH inequality, $|\langle S_{\text{CHSH}}\rangle| \leq 2$.

The canonical example in which quantum mechanics violates this inequality is where Alice and Bob each possess one part of the maximally entangled 2-qubit singlet state, $|\Psi^-\rangle = (|0\rangle_A \otimes |1\rangle_B - |1\rangle_A \otimes |0\rangle_B)/\sqrt{2}$. The CHSH parameter becomes the operator

$$\hat{S}_{\text{CHSH}} = (\hat{X}+\hat{Z}) \otimes \hat{P} + (\hat{X}-\hat{Z}) \otimes \hat{Q}. \tag{3}$$

To maximize violation of the CHSH inequality [21], Alice chooses to measure from the Pauli bases $\hat{X} \equiv |0\rangle\langle 1| + |1\rangle\langle 0|$, $\hat{Z} \equiv |0\rangle\langle 0| - |1\rangle\langle 1|$, and Bob from the bases $\hat{P} \equiv -(\hat{Z}+\hat{X})/\sqrt{2}$ and $\hat{Q} \equiv (\hat{Z}-\hat{X})/\sqrt{2}$. A simple calculation yields $|\langle\hat{S}_{\text{CHSH}}\rangle| = |\text{Tr}[\hat{S}_{\text{CHSH}}\,|\Psi^-\rangle\langle\Psi^-|]| = 2\sqrt{2}$, violating the CHSH inequality by a factor of $\sqrt{2}$.

The key feature of weak measurements is that they minimize measurement back-action. This allows measurement results to be obtained for all four variables (X, Z, P, and Q) for the same two-qubit system simultaneously. For example, weak measurements can be performed in the $\hat{Z}$ basis on system A and in the $\hat{Q}$ basis on system B, before strongly measuring the systems in the $\hat{X}$ and $\hat{P}$ bases respectively. Through this process one can determine $|\langle\hat{S}_{\text{CHSH}}\rangle|$ using fixed measurements on every system in the ensemble.

The measurement results have large variance due to the weak coupling of the measurement device to the system. However, the formalism of weak values allows us to extract a reliable, observationally justified value for the observables weakly measured on the ensemble. Within the overall ensemble of states with a given preparation, subensembles of systems can be defined by postselection, i.e. by the outcome of the final strong measurement. For each such subensemble, the average value of the results of the weak intermediate measurement, of some observable $\hat{O}$ in general, is known as the *weak value* [22] of $\hat{O}$ over that subensemble, and represents an empirically relevant way to talk about the value of $\hat{O}$ between preparation and measurement. For qubits, every Hermitian operator is proportional to the identity plus a projector; the former has a weak value of one, and the latter has a weak value that can be termed a *weak-valued probability*, $\Pr^{\text{w}}$, for the eigenvalue associated with that projector. That is, for qubits, every measurement of a weak value is equivalent to measuring a weak-valued probability [23].

To see how this is applied to the CHSH inequality, first consider the weak measurement in the $\hat{Z}$ basis of a single qubit in a state $|\psi\rangle$, followed by a strong measurement in $\hat{X}$, which we can state as a postselection of the measurement eigenstate $|\phi(x)\rangle$ corresponding to the result x. For this postselected ensemble, the weak value, given by [16]

$$_{\phi}\langle\hat{Z}\rangle^{\text{w}}_{\psi} \equiv \text{Re}\left[\frac{\langle\phi(x)|\hat{Z}|\psi\rangle}{\langle\phi(x)|\psi\rangle}\right], \tag{4}$$

quantifies the expectation value of the results of weak measurements in the $\hat{Z}$ basis, as the measurement strength goes to zero. Weak values are unusual in that they can take values outside the spectrum of the measurement operator, but are nevertheless useful in increasing measurement precision where the resolution of the measuring device is otherwise the limiting factor [24–28], and in resolving a number of quantum mechanical paradoxes (e.g. refs. [16, 17, 29–35]) and investigating macrorealism on one [36, 37] or two [38] systems.

If we now consider the $\hat{Z}$ basis projectors, $\hat{\Pi}_z$, the weak value $_{\phi}\langle\hat{\Pi}_z\rangle^{\text{w}}_{\psi}$ can be interpreted as a weak-valued probability of obtaining the outcome z, given the $|\psi\rangle$ input state, conditional on finally postselecting the $|\phi(x)\rangle$ state indicating an outcome x in the $\hat{X}$ basis, i.e. $\Pr^{\text{w}}[z|x,\psi] = {}_{\phi}\langle\hat{\Pi}_z\rangle^{\text{w}}_{\psi}$. Because the back-action imparted onto the system by the weak measurement is negligible, it follows that the joint probability of obtaining both $X = x$ and $Z = z$ outcomes is therefore

$$\Pr^{\text{w}}[x,z|\psi] = {}_{\phi}\langle\hat{\Pi}_z\rangle^{\text{w}}_{\psi}\Pr[\phi(x)|\psi], \tag{5}$$

where $\Pr[\phi(x)|\psi] = |\langle\phi(x)|\psi\rangle|^2$. Weak measurements thereby allow us to ascertain (pseudo-) probabilities for outcomes that are not directly obtainable by typical measurements.

Similarly, the joint probabilities for the two-qubit case can also be found:

$$\Pr^{\text{w}}[x,z,p,q|\psi] = {}_{\phi}\langle\hat{\Pi}_z \otimes \hat{\Pi}_q\rangle^{\text{w}}_{\psi}\Pr[\phi(x,p)|\psi], \tag{6}$$

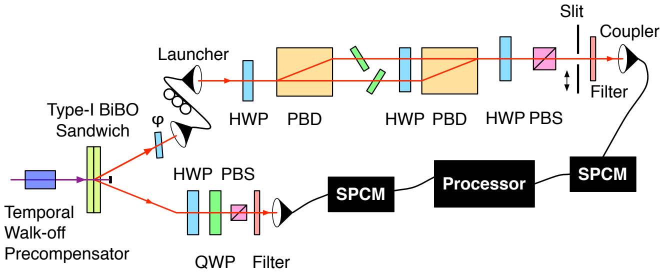

FIG. 2: Experimental apparatus. Pairs of entangled photons are generated by a type-I bismuth borate (BiBO) 'sandwiched pair' source. One of the photons undergoes strong measurement, the other is coupled to single-mode optic fibre and directed to the weak measurement apparatus, implemented as a polarization interferometer. A tilted optical plate is placed in each interferometric arm, causing a polarization-dependent transverse shift of the spatial Gaussian mode of the photon, with polarization postselection following. The mode intensity is sampled by a scanning slit, and is collected into a multimode optical fibre (after passing through telescoping lenses, not shown). Processing the single-photon counting module (SPCM) detection rates completes the weak measurement.

where $\hat{\Pi}_q$ represents projectors in the $\hat{Q}$ basis (applied here to Bob's qubit) corresponding to the outcome q, and the postselection state $|\phi(x,p)\rangle$ depends on strong measurement outcomes of both Alice's ($X = x$) and Bob's ($P = p$) qubits.

We can thus calculate the weak-valued joint probabilities of each of the 16 outcomes of measurements on the entangled state $|\Psi^-\rangle$. They each take one of the four possible values: $(2+\sqrt{2})/16$, $\sqrt{2}/16$, $(2-\sqrt{2})/16$, and $-\sqrt{2}/16$. Of particular note are the conditions for each of the two possible outcomes for the CHSH parameter, $S_{\mathrm{CHSH}} = \pm 2$. We find that the total probability for the positive outcome is $(1+\sqrt{2})/2 \approx 1.207$, while the probability for the negative outcome is $(1-\sqrt{2})/2 \approx -0.207$. It is easy to see that the contribution to the expectation value, equation (2), is therefore positive in both cases, giving $|\langle S_{\mathrm{CHSH}}\rangle| = 2\sqrt{2}$ as expected [19].

These non-realistic (i.e. outside the range $[0,1]$) probabilities may at first seem nonsensical. Indeed, they cannot be measured as relative frequencies in the laboratory—instead they must be inferred from weak measurement data, as we do below. They arise simply from the fact that they stand for strong measurement results which cannot be physically obtained (events that cannot actually take place) because of measurement back-action. As shown previously [34, 35, 39], such non-realistic probabilities are nevertheless useful in probability accounting for physically realizable events.

We now present an experimental demonstration of these non-realistic probabilities using photons. Firstly we note that if Alice could obtain both X and Z measurement results simultaneously, then by equation (1) either P or Q of Bob's results would not matter for each shot. The only empirically relevant weak-valued probabilities are then either $\Pr^{\mathrm{w}}[x,z,p]$ or $\Pr^{\mathrm{w}}[x,z,q]$. We may therefore simplify the experiment by performing weak measurement of only one photon of each pair (Alice's), rather than both simultaneously, with the probabilities for each outcome of the CHSH parameter remaining unchanged.

Pairs of photons entangled in polarization and having high fidelity with $|\Psi^-\rangle$ are generated via spontaneous parametric downconversion (using a type-I 'sandwiched pair' source [40]; see the Appendix). One photon of the downconverted pair is assigned to Bob and immediately undergoes a strong measurement, either $\hat{P}$ or $\hat{Q}$, by postselection using a quarter-wave plate (QWP), half-wave plate (HWP), and polarizing beamsplitter (PBS). The other photon is assigned to Alice, coupled to a single-mode optical fibre, and guided to the weak measurement apparatus. Photons exit the single-mode fibre and pass through a collimating lens, resulting in a Gaussian mode. Photons then pass through a HWP at its optic axis. Weak measurements are achieved by engineering a polarization-dependent displacement, Δr, significantly smaller than the width of the transverse Gaussian mode [41].

To achieve this displacement, we construct a partially spatially-mismatched polarization interferometer. A polarizing beam displacer (PBD) separates the horizontal and vertical polarizations of the photon into two parallel spatial modes. An optical plate is placed in each mode and tilted in approximately equal opposing directions, causing small opposite displacements of the two modes following Snell's law. A HWP flips horizontal and vertical polarizations of the photon, the modes of which then (partially) recombine by the final PBD. Despite the interferometric modes not perfectly overlapping, a large Gaussian beam width relative to the size of the displacement ensures that decoherence (i.e. measurement back-action) is negligible. The photon is then postselected in the conjugate basis using a HWP at ±22.5° from its optic axis followed by a PBS. A slit, seated on a motorized translation stage, is scanned in the direction transverse to the beam, allowing us to sample the photon flux of the Gaussian profile at any point r within the range of the stage (25 mm). Integration of the photon flux (in coincidence with Bob's photons) allows us to determine the expectation of the weak polarization measurement. The joint probability of each polarization outcome of Alice's and Bob's photons can then be inferred (see the Appendix). Assigning horizontal and vertical polarizations to the $Z = +1$ and $Z = -1$ states, respectively, we thus obtain weak measurements in the $\hat{Z}$ basis, with postselection in the $\hat{X}$ basis.

The performance of the photon source is quantified by conducting quantum state tomography [42] with the slit removed and a QWP inserted immediately before the final HWP. With a two-photon state of measured

Bell-state fidelity 0.948 ± 0.002 and tangle [43] 0.841 ± 0.004, we expect to be able to achieve a CHSH value of $|\langle S_{\mathrm{CHSH}} \rangle| \approx 2.67$, sufficient to violate the CHSH inequality. For this state, the experimentally determined weak-valued probabilities are 1.172 ± 0.008 for $S_{\mathrm{CHSH}} = +2$ and -0.171 ± 0.002 for $S_{\mathrm{CHSH}} = -2$, resulting in $|\langle S_{\mathrm{CHSH}} \rangle| = 2.686 \pm 0.017$ and violating the CHSH inequality by more than 40 standard deviations.

Our choice of weakly measuring in the $\hat{Z}$ basis is arbitrary—we may instead measure $\hat{X}$ weakly before a strong $\hat{Z}$ measurement and obtain essentially identical expected joint probabilities. To demonstrate this, we introduce a change of basis of the measurements by setting the initial HWP in the weak measurement device to 22.5° from its optic axis. Performing the experiment in this condition we find a tangle of 0.857 ± 0.005, and probabilities of 1.147 ± 0.008 for $S_{\mathrm{CHSH}} = +2$ and -0.140 ± 0.002 for $S_{\mathrm{CHSH}} = -2$. This gives a CHSH value of 2.574 ± 0.016. Despite the improved tangle for this state, sensitivity to imprecision in the manual setting of the change-of-basis HWP leads to slightly reduced magnitudes of the measured probabilities.

With weak measurements in the $\hat{Z}$ basis, we also perform the experiment for states of various tangle, obtained by tuning the source (see the Appendix). The results, shown in Figure 3(**a**), demonstrate beyond-unit and negative probabilities for states with high tangle (above $3 - 2\sqrt{2} \approx 0.17$), with magnitudes decreasing with tangle. Violation of the CHSH bound is also seen for these states (Figure 3(**b**)). States with tangle below ≈0.17 do not exhibit these non-realistic probabilities. This corresponds to the CHSH value for these states passing below the bound of 2. (Any pure state with nonzero tangle can violate the CHSH inequality [43], however this requires optimization of the measurement bases, which we do not do here.)

For our apparatus, the results that we measure can be reproduced by a local hidden variable (LHV) theory; this is the case with any protocol in which there is no measurement choice on one side. However, the weak measurement formalism allows us to extract strong-measurement joint probabilities which cannot be reproduced by any LHV theory. While standard CHSH tests may also be explained by recourse to negative joint probabilities (by assuming that equation (2) always holds and $X, Z, P, Q \in \{\pm 1\}$), there is no a priori reason to expect such negative joint probabilities to have an experimental significance. In our weak measurement scheme, the negative joint probabilities naturally arise as the outcomes of experiments probing the intermediate state of the system.

Furthermore, the non-realistic probabilities arising from our weak measurement approach connect to a framework in which even entangled states can be described in a local way. Specifically, entangled states can be written as a statistical sum of local 'transient' states [15], i.e. in the form $\hat{\rho}_i = \sum_f \Pr[f|i] \hat{R}_{if}$, where $\hat{R}_{if}$ is a *separable* matrix—a tensor product of matrices describing each qubit separately—as discussed by Hofmann [15, 19]. The transient density matrices $\hat{R}_{if}$ completely represent the state as it transits from preparation in state $\hat{\rho}_i$ to final measurement described by separable two-qubit POVM elements $\{\hat{F}_f\}$, yielding outcome f (reference [15]). They are given by

$$\hat{R}_{if} = \frac{\hat{F}_f \hat{\rho}_i + \hat{\rho}_i \hat{F}_f}{2\,\mathrm{Tr}[\hat{F}_f \hat{\rho}_i]}. \tag{7}$$

Each satisfies two of the three conditions for an ordinary density matrix: it is Hermitian with unit trace. However they may violate the third condition (positivity) by possessing negative eigenvalues. Nevertheless, these transient density operators provide empirically verifiable predictions of measurement results.

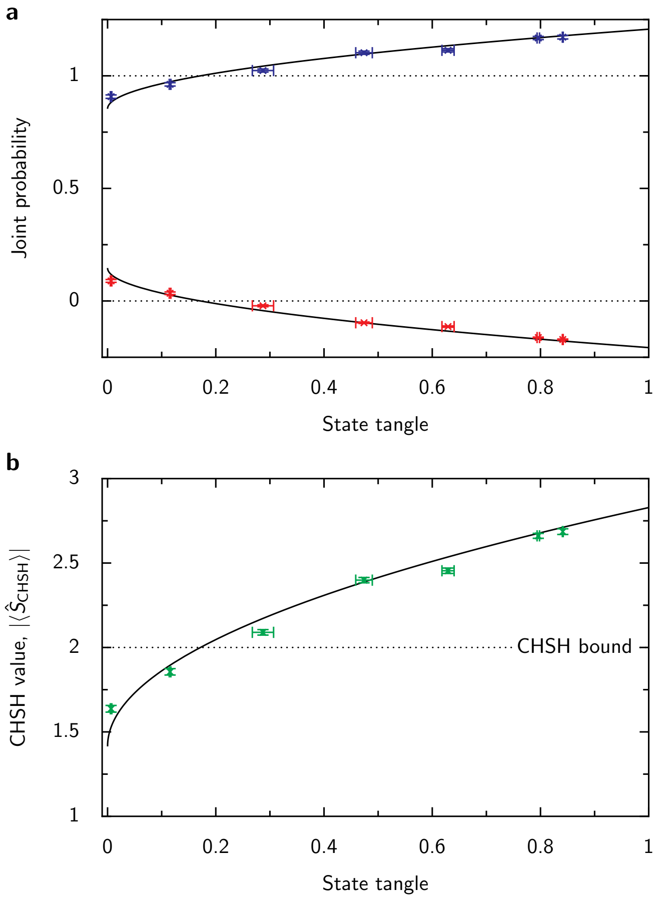

FIG. 3: Experimental results for states of various tangle. **a,** Joint probabilities of the outcomes corresponding to $S_{\mathrm{CHSH}} = 2$ (upper curve) and $S_{\mathrm{CHSH}} = -2$ (lower curve). **b,** The CHSH value $|\langle \hat{S}_{\mathrm{CHSH}} \rangle|$ calculated using the joint probabilities. The experimentally measured values (points) closely match the ideal theoretical values (lines) as the tangle of the state varies. Horizontal error bars represent the range of tangles measured via tomography taken before and after data collection. Vertical error bars span one standard deviation.

We used our strong measurement tomography of the input state $\hat{\rho}_i$ to construct the various $\hat{R}_{if}$ for our experiment, using equation (7). From these, it is possible to derive the joint measurement probabilities $\mathrm{Pr}^{\mathrm{w}}[S_{\mathrm{CHSH}} = +2]$ and $\mathrm{Pr}^{\mathrm{w}}[S_{\mathrm{CHSH}} = -2]$, which we compared with the experimental joint probabilities found with weak measurements. From the $\hat{R}_{if}$ representation of the most entangled state in Figure 3 (tangle 0.841), we found $\mathrm{Pr}^{\mathrm{w}}[S_{\mathrm{CHSH}} = +2] = 1.168 \pm 0.002$ and $\mathrm{Pr}^{\mathrm{w}}[S_{\mathrm{CHSH}} = -2] = -0.168 \pm 0.002$, within two standard deviations of the weak measurement experimental results. We also found good agreement for all other tested states.

As a result of equation (7), the weak values framework suggests an interpretation of Bell inequality violations in which the assumption of locality is retained and that of realism is discarded. This is because the measurement result f simply selects, out of the statistical distribution, one of the *local* subensembles $\hat{R}_{if}$, which completely characterizes the coherences present in $\hat{\rho}_i$. Therefore, correlations in two-qubit measurement outcomes do not correspond to nonlocal action, but rather result from a classical Bayesian updating of probabilities. On the other hand, the negative eigenvalues of the transient density matrix indicate that the system does not possess a realistic state prior to the final measurement.

By exploiting the power of weak measurements, we have presented an experimental violation of the CHSH inequality in terms of non-realistic weak-valued probabilities which align with a local interpretation of quantum mechanics. Our results point the way to further novel investigations of fundamental quantum phenomena in which typical strong measurements are replaced with weak measurements, possessing as little back-action as desired. As with the CHSH inequality shown here, this approach could offer deep insights into the most puzzling aspects of quantum mechanics.

We thank Holger Hofmann for helpful discussions. This work was supported by the Australian Research Council.

[1] M. Nielsen and I. Chuang, *Quantum Computation and Quantum Information* (Cambridge Univ. Press, Cambridge, UK, 2000).
[2] R. Horodecki, P. Horodecki, M. Horodecki, and K. Horodecki, Rev. Mod. Phys. **81,** 865–942 (2009).
[3] T. D. Ladd *et al.*, Nature **464,** 45–53 (2010).
[4] A. Zeilinger, *Dance of the Photons: From Einstein to Teleportation* (Farrar, Straus and Giroux, 2010).
[5] H. M. Wiseman and G. J. Milburn, *Quantum Measurement and Control* (Cambridge Univ. Press, Cambridge, 2010).
[6] A. Einstein, B. Podolsky, and N. Rosen, Phys. Rev. **47,** 777 (1935).
[7] J. S. Bell, Physics **1,** 195–200 (1964).
[8] S. J. Freedman and J. F. Clauser, Phys. Rev. Lett. **28,** 938–941 (1972).
[9] A. Aspect, P. Grangier, and G. Roger, Phys. Rev. Lett. **49,** 91–94 (1982).
[10] A. Aspect, J. Dalibard, and G. Roger, Phys. Rev. Lett. **49,** 1804–1807 (1982).
[11] G. Weihs, T. Jennewein, C. Simon, H. Weinfurter, and A. Zeilinger, Phys. Rev. Lett. **81,** 5039–5049 (1998).
[12] P. G. Kwiat, E. Waks, A. G. White, I. Applebaum, and P. H. Eberhard, Phys. Rev. A **60,** 2 (1999).
[13] D. Salart, A. Baas, J. A. W. van Houwelingen, N. Gisin, and H. Zbinden, Phys. Rev. Lett. **100,** 220404 (2008).
[14] T. Scheidl *et al.*, P. Natl. Acad. Sci. USA **107,** 19708–19713 (2010).
[15] H. F. Hofmann, Phys. Rev. A **81,** 012103 (2010).
[16] H. M. Wiseman, Phys. Rev. A **65,** 032111 (2002).
[17] S. Kocsis, *et al.*, Science **332,** 1170–1173 (2011).
[18] J. S. Lundeen, B. Sutherland, A. Patel, C. Stewart, and C. Bamber, Nature **474,** 188–191 (2011).
[19] H. F. Hofmann, arXiv:0911.0071 (2009).
[20] J. F. Clauser, M. A. Horne, A. Shimony, and R. A. Holt, Phys. Rev. Lett. **23,** 880–884 (1969).
[21] B. S. Cirel'son, Lett. Math. Phys. **4,** 93 (1980).
[22] Y. Aharonov, D. Z. Albert, and L. Vaidman, Phys. Rev. Lett. **60,** 1351 (1988).
[23] A. P. Lund and H. M. Wiseman, New J. Phys. **12,** 093011 (2010).
[24] O. Hosten and P. Kwiat, Science **319,** 787–790 (2008).
[25] P. B. Dixon, D. J. Starling, A. N. Jordan, and J. C. Howell, Phys. Rev. Lett. **102,** 173601 (2009).
[26] N. Brunner and C. Simon, Phys. Rev. Lett. **105,** 010405 (2010).
[27] D. J. Starling, P. B. Dixon, A. N. Jordan, and J. C. Howell, Phys. Rev. A **82,** 063822 (2010).
[28] H. F. Hofmann, M. E. Goggin, M. P. Almeida, and M. Barbieri, arXiv:1107.4735, (2011).
[29] A. M. Steinberg, Phys. Rev. Lett. **74,** 2405–2409 (1995).
[30] K. J. Resch and A. M. Steinberg, Phys. Rev. Lett. **92,** 130402 (2004).
[31] N. Brunner, V. Scarani, M. Wegmüller, M. Legré, and N. Gisin, Phys. Rev. Lett. **93,** 203902 (2004).
[32] K. J. Resch, J. S. Lundeen, and A. M. Steinberg, Phys. Lett. A **324,** 125–131 (2004).
[33] G. J. Pryde, J. L. O'Brien, A. G. White, T. C. Ralph, and H. M. Wiseman, Phys. Rev. Lett. **94,** 220405 (2005).
[34] R. Mir *et al.*, New J. Phys. **9,** 287 (2007).
[35] J. S. Lundeen and A. M. Steinberg, Phys. Rev. Lett. **102,** 020404 (2009).
[36] N. S. Williams and A. N. Jordan, Phys. Rev. Lett. **100,** 026804 (2008).
[37] M. E. Goggin *et al.*, Proc. Natl. Acad. Sci. **108,** 1256 (2011).
[38] J. Dressel, C. J. Broadbent, J. C. Howell and, A. N. Jordan, Phys. Rev. Lett. **106,** 040402 (2011).
[39] R. P. Feynman, *Negative Probabilities.* pp. 235–248. Quantum Implications: Essays in honour of David Bohm. (Routledge, New York 1991).
[40] R. Rangarajan, M. Goggin, and P. Kwiat, Opt. Express **17,** 18920 (2009).
[41] N. W. M. Ritchie, J. G. Story, and R. G. Hulet, Phys. Rev. Lett. **66,** 1107–1110 (1991).
[42] J. B. Altepeter, D. F. V. James, and P. G. Kwiat, Lect. Notes Phys. **649,** 113–145 (2004).
[43] W. J. Munro, K. Nemoto, and A. G. White, J. Mod. Opt. **48,** 1239–1246, 2001.

Appendix

Experimental joint probabilities

Let r_H represent the centroid of the Gaussian profile associated with horizontally polarized photons exiting the interferometer, and r_V represent the centroid of vertically polarized photons. Because $r_V > r_H$ in our apparatus, it is convenient to write the displacement $\Delta r = r_V - r_H$. With horizontal polarization corresponding to $Z = +1$ and vertical polarization corresponding to $Z = -1$, measuring the position of the Gaussian profile for a given photon state corresponds to a $\hat{Z}$ measurement. In typical spatial-mode qubit encodings, the modes are sufficiently far apart that the Guassian profiles are approximately orthogonal, and the measurement outcomes thus correspond to strong measurements. The expectation value for these measurements may be written

$$\langle \hat{Z} \rangle = \int_{-\infty}^{\infty} \frac{r_H + r_V - 2r}{\Delta r} \wp(r)\, dr, \qquad \text{(A.8)}$$

where $\wp(r)$ is the (Gaussian) probability density of detecting a photon at a position r. (For notational convenience, we omit the explicit dependence on the initial state $|\psi\rangle$.) As Δr is reduced towards zero, the measurement becomes weak and the uncertainty of individual outcomes increases due to the overlapping Gaussian distributions for each outcome. In the absence of postselection, however, the expectation value is the same in both the weak and strong measurement cases. Therefore,

$$\sum_z z \Pr^{\mathrm{w}}[z] = \int_{-\infty}^{\infty} \frac{r_H + r_V - 2r}{\Delta r} \wp(r)\, dr. \qquad \text{(A.9)}$$

Using the fact that the two weak-valued probabilities in equation (A.9) must sum to one, it follows immediately that

$$\Pr^{\mathrm{w}}[Z = +1] = \frac{1}{\Delta r} \int_{-\infty}^{\infty} (r_V - r) \wp(r)\, dr, \qquad \text{(A.10)}$$

and

$$\Pr^{\mathrm{w}}[Z = -1] = \frac{1}{\Delta r} \int_{-\infty}^{\infty} (r - r_H) \wp(r)\, dr. \qquad \text{(A.11)}$$

The postselection outcomes become extra conditions on equations (A.10) and (A.11). Supposing Bob measures $\hat{P}$, Alice $\hat{X}$, then $\wp(r)$ becomes $\wp(r)\Pr[x,p]$, and $\Pr^{\mathrm{w}}[z]$ becomes $\Pr^{\mathrm{w}}[z,x,p]$. The joint probabilities can be calculated from experimental counting statistics by considering equations (A.10) and (A.11). For a finite slit width, the integral becomes a sum approximation over the range of measured positions as dr becomes δr,

$$\Pr^{\mathrm{w}}[Z = +1, x, p] \approx \frac{1}{\Delta r} \sum_r (r_V - r) \wp(r) \Pr[x,p] \delta r, \qquad \text{(A.12)}$$

and similarly for $\Pr^{\mathrm{w}}[Z = -1, x, p]$.

The value of $\wp(r)\Pr[x,p]$ cannot be measured directly, but must instead be estimated from photon detections. Let $C(r,x,p)$ represent the count rate of these detections. Then $\wp(r)\Pr[x,p]\delta r = C(r,x,p)/C_{\mathrm{T}}$, where $C_{\mathrm{T}} = \sum_{r,x,p} C(r,x,p)$ is the total number of coincident photon detections over all the outcomes of the measurements in $\hat{X}$ and $\hat{P}$. The joint probability can therefore be estimated by

$$\Pr^{\mathrm{w}}[Z = +1, x, p] \approx \frac{\sum_r (r_V - r) C(r,x,p)}{\Delta r \sum_{r,x,p} C(r,x,p)}, \qquad \text{(A.13)}$$

and similarly for $\Pr^{\mathrm{w}}[Z = -1, x, p]$, $\Pr^{\mathrm{w}}[Z = +1, x, q]$, and $\Pr^{\mathrm{w}}[Z = -1, x, q]$. The probabilities of the positive and negative outcomes of the CHSH parameter are determined by taking the appropriate sums of these results.

Source

Photons pairs entangled in polarization are generated using a type-I bismuth borate (BiBO) spontaneous parametric downconversion 'sandwiched pair' source [40], pumped by 410 nm light from a mode-locked frequency-doubled Ti:sapphire laser. Two thin (0.6 mm) BiBO crystals, one cut for downconversion of horizontally polarized incident light, the other cut for vertically polarized incident light, are placed back-to-back. Pumping by diagonally polarized light induces coherent downconversion from the two crystals resulting in the two-photon polarization state $(|H\rangle|H\rangle + e^{i\varphi}|V\rangle|V\rangle)/\sqrt{2}$, for some constant phase φ. By changing the polarization of the pump light we can adjust the proportion satisfying the phase matching conditions of each crystal, thereby tuning the degree of entanglement generated. For a pump polarization angle θ, the resulting state is $|\psi(\theta)\rangle = \sin\theta\,|H\rangle|H\rangle + e^{i\varphi}\cos\theta\,|V\rangle|V\rangle$ with a tangle of $\sin^2 2\theta$.

Each photon of the generated pair is assigned to either Alice or Bob. Before being coupled to a single-mode optical fibre, Alice's photon passes through a HWP set to its optic axis. This HWP is tilted around vertical such that it compensates for φ and achieves a state having high fidelity with $|\Psi^-\rangle$ at the measurement apparatus (in the condition of a diagonally polarized pump beam).

Photon measurement

The photon assigned to Alice undergoes weak measurement through polarization-dependent transverse displacement caused by tilted optical plates. For our apparatus it was logistically convenient to use quarter-wave plates set at their optic axes. Upon successful postselection the photon then arrives at the scanning slit, after which the photon passes through telescoping lenses (not shown in Figure 2), a 3 nm full width half maximum interference filter, and is coupled into a multi-mode fibre guided to a single-photon counting module (SPCM). Similarly, following postselection, Bob's photon also passes through a 3 nm interference filter, and is coupled into a single-mode optical fibre guided to a SPCM. Alternatively to postselection, one could also perform strong two-outcome polarization measurements. Neither the polarization filtering method that we use, nor the slit-induced spatial filtering, are fundamental.

Coincidence counting

Detecting Bob's and Alice's photons within a coincidence window of ≈3 ns helps ensure high-fidelity entangled two-photon states, however some accidental coincident detections remain. We estimate these accidental count rates by simultaneously recording detection events of the two SPCMs coincident when displaced in time by the pump pulsing period. All such detections thus arise from uncorrelated events. We subtract these accidental coincident counts from our results.

Data collection

We use a slit of width approximately 350 µm, scanned over a 3.5 mm range in steps of 87.5 µm, counting for 10 s at each step. This is performed for each of the eight total postselections for X, P, and Q, in turn. The process is repeated 70 times, ensuring that any drift in pump power is experienced equally (approximately) for each outcome. To calculate the joint probabilities it is necessary to characterize the centroid positions r_H and r_V. This is done by additionally postselecting horizontal and vertical photon polarization states, making a total of ten measurement conditions in the experiment. We fit a Gaussian function to the count rates of each characterization—the centres of these fits define r_H and r_V.